Gating of the Squid Sodium Channel at Positive Potentials. I. Macroscopic Ionic and Gating Currents.

Ana M. Correa and Francisco Bezanilla
Department of Physiology, School of Medicine, University of California at Los Angeles, Los Angeles, CA 90024, and Marine Biological Laboratory, Woods Hole, MA 02543

ABSTRACT Macroscopic ionic sodium currents and gating currents were studied in voltage-clamped, dialyzed giant axons of the squid *Loligo pealei* under conditions of regular and inverse sodium gradients. Sodium currents showed regular kinetics but inactivation was incomplete, showing a maintained current for depolarizations lasting 18 ms. The ratio of the maintained current to the peak current increased with depolarization and it did not depend on the direction of the current flow or the sodium gradient. The time constant of inactivation was not affected by the sodium gradient. Double-pulse experiments allowed the separation of a normal inactivating component and a noninactivating component of the sodium currents. In gating current experiments, the results from double-pulse protocols showed that the charge was decreased by the prepulse and that the slow component of the 'on' gating current was preferentially depressed. As expected, charge immobilization was established faster at higher depolarizations than at low depolarizations, however, the amount of immobilized charge was unaffected by the pulse amplitude. This indicates that the incomplete sodium inactivation observed at high depolarizations is not the result of decreased charge immobilization; the maintained current must be due to a conductance that appears after normal charge immobilization and fast inactivation.

INTRODUCTION

In the squid giant axon, a depolarizing stimulus brings about a fast transient sodium current that further depolarizes the membrane and, with a small delay, a repolarizing potassium current (Hodgkin and Huxley, 1952). The peak of the sodium current is reached within the first couple of milliseconds and then decays in about 10 ms. The rising phase of this inward current is due to the process of activation, brought about by the depolarization, which opens the sodium conductance allowing current flow driven by the difference between the membrane potential and the sodium equilibrium potential. The decay of the current, brought about by the process called inactivation, is essentially a shutdown of the conductance while the membrane is still depolarized (Hodgkin and Huxley, 1952). With the advent of single-channel recording (Hamill et al., 1981) it became possible to study the sodium conductance at the single molecule level. Many of the features of the sodium conductance can be interpreted as the average behavior of single channels. Activation opens the channels, and inactivation makes the channels nonconductive again, safeguarding the membrane from repetitive and continuous depolarization. The squid sodium channel opens with a slight lag upon depolarization, and, after several closures and reopenings, it finally closes due to the establishment of inactivation (Bezanilla, 1987; Vandenberg and Bezanilla, 1991a, b). The rates at which these steps take place and the number of states in which a Na^+ channel dwells before actually reaching an open configuration vary depending on the particular preparation studied, and, as a consequence, the subject has not been devoid of controversy. One consistent finding has been the prevalence of a single open state (i.e., Quandt and Narahashi, 1982; Horn and Vandenberg, 1984; Scanley et al., 1990). However, data supporting more than one open state in sodium channels has been reported in frog Node of Ranvier (Sigworth, 1981) and in N1E 115 neuroblastoma cells (Nagy et al., 1983; Nagy, 1987). For the particular case of the squid sodium channel, more than one conductance was proposed by Chandler and Meves (1970a–c) and by Bezanilla and Armstrong (1977) to explain certain features of the sodium conductance. In this and the accompanying paper we present evidence for a second open state in the squid giant axon sodium channel; this second open state would get populated mainly at very positive potentials and explains the incomplete inactivation observed at these potentials, an observation in experiments more frequently done under conditions of inverse gradient (Chandler and Meves, 1970a–c; Keynes et al., 1992a, b; Keynes and Meves, 1993).

Ever since the early work in the squid giant axon (Adelman and Senft, 1966) and, in particular, with the work by Chandler and Meves (1970a–c) it has been known that at very positive potentials with high sodium inside the sodium current does not completely subside during the depolarizing pulse. Instead, there is a remnant steady level that is more obvious the more depolarized the potential. This plateau current was later found to be a property of the squid sodium currents also seen in nonperfused axons (Shoukimas and French, 1980). More recent work by Keynes and collaborators, (1992a, b; 1993) has further characterized some unique features of each of the apparent two components of

Received for publication 10 November 1993 and in final form 15 March 1994.

Address reprint requests to Ana M. Correa, Department of Physiology, UCLA School of Medicine, 10833 Le Conte Avenue, Los Angeles, California 90024-1751.

0006-3495/94/06/1853/11 $2.00

the currents, one that inactivates and another that does not inactivate. There were questions posed by Chandler and Meves, the answer to which we have only recently been able to confirm due to the opportunity given by patch clamp studies to observe single-channel molecules. The main two questions were: are these two different conductances (or channels), or is it a property of the same channel (for example, more than one open state)? And, to what extent is the lasting, noninactivating current a consequence of high concentrations of sodium in the inside? In reference to the latter, Shoukimas and French (1980) showed that incomplete inactivation also occurred in nonperfused axons, indicating that it was not due only to the high internal sodium used in the perfusates. The evidence we have accumulated with ionic macroscopic gating and single-channel currents supports the hypothesis that it is a single type of sodium channel that is responsible for the behavior at very positive potentials irrespective of the orientation of the current flow. The present paper deals with macroscopic ionic and gating currents obtained from dialyzed squid giant axons. The results from single-channel recordings are presented in the following paper (Correa and Bezanilla, 1994). Preliminary results have been previously presented (Bezanilla and Correa, 1992).

MATERIALS AND METHODS

Squid axons

All the experiments were done in giant axons of the squid *Loligo pealei* obtained at the Marine Biological Laboratories, in Woods Hole, MA. Axons were dissected in sea water, cleaned of connective tissue under the dissecting microscope, and transferred to the recording chamber. The procedure to record from a dialyzed axon has been described previously in detail (Perozo et al., 1989). The dialysis cannula had a molecular weight cut-off of 9000 Da. All the experiments were done at low temperature (5°C).

Solutions

Ionic Currents

In the text and figure legends the convention "external//internal," was used when referring to the composition of the solutions. For most of the experiments done with an inverse sodium gradient, the external solution was 0 Na^+ choline sea water (0 Na^+ CSW): 530 mM choline-Cl, 10 mM $CaCl_2$, 10 mM HEPES, and *N*-Methyl-D-glucamine (NMG), pH 7.2. The dialysis medium was a dilution of an internal high sodium solution (535 Na^+: 500 mM Na-glutamate, 10 mM NaCl, 20 mM NaF, 1 mM EGTA-Cs, and 10 mM HEPES-Na, pH 7.3) with an internal Cs^+ gating current dialysis solution with no Na^+ (see below). The final sodium concentration in the high internal sodium medium was 178 mM. Notice that this dialysis solution contained 93 mM Cs^+, hence the name, 178 Na^+-93 Cs^+. For experiments done with a normal sodium gradient, the external solution was also made by dilution of a high sodium external solution (540 Na^+: 540 mM NaCl, 10 mM HEPES-Na, pH 7.6) with 0 Na^+ CSW. In this case the external sodium was 108 mM. The internal medium was normally the internal NMG^+ or Cs^+ gating dialysis media, which contain no Na^+ (see below).

Gating Currents

For gating current experiments, 1 μM tetrodotoxin (TTX) was added to the external solution. During gating current experiments the internal solutions were normally the internal NMG^+ or Cs^+ gating dialysis media, which contained 140 mM NMG (or Cs)-F, 50 mM tetraethylammonium (TEA)-glutamate, 12.5 mM EGTA-NMG (or Cs), 10 mM HEPES-NMG (or Cs), pH 7.3, and 470 sucrose. The external medium was 0 Na^+ CSW. In some inverse gradient experiments, however, the high sodium internal dialysate was maintained during gating current recordings.

Recordings

All currents were recorded only after the baseline and ionic current levels were stable. Subtraction records were recorded after each ionic current experiment by reproducing the various pulse protocols in the presence of TTX to block the ionic currents. Series resistance compensation was used in all experiments. Gating currents were recorded following the P/4 or P/−4 procedures (Bezanilla and Armstrong, 1977). Several trials, normally 20, were averaged per record. The subtracting holding potentials were −140 or −150 mV. The experimental setup was similar to that described by Stimers et al. (1985). Filter bandwidths were 25 kHz for ionic currents and 50 kHz for gating.

RESULTS

Ionic currents

In Fig. 1 (*top*) are representative records of sodium currents obtained in a dialyzed squid giant axon at positive potentials and with an inverse sodium gradient (0 Na^+ CSW//178 Na^+). The outward currents elicited under these conditions show the basic features of typical sodium currents: they activate promptly with depolarization within the first couple of ms, they reach a peak and then decline due to the process of inactivation. In contrast to the regular sodium currents normally obtained in the negative range of potentials, inactivation here is less complete, leaving a considerable, remnant steady-state component (I_{ss}) at the end of the pulse. The magnitudes of the peak and the steady-state currents are better compared in Fig. 2. In panel *A* are plotted the current to voltage (I-V) relations under inverse gradient conditions at the peak of the current and at the end of the pulse for potentials from −40 to +100 mV. Also plotted is the instantaneous I-V for the same axon. Under these ionic conditions

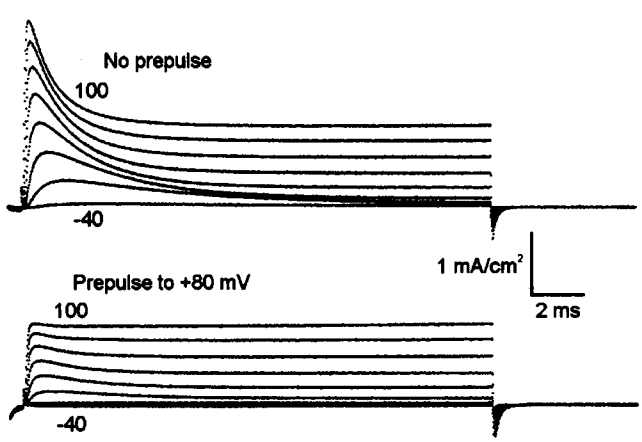

FIGURE 1 Macroscopic outward sodium currents obtained in an axon dialyzed with 178 mM Na^+-93 mM Cs^+ in external choline sea water (0 Na^+ CSW). Top: Family of traces from −40 to +100 mV every 20 mV. Bottom: The same family of traces after depolarizing prepulses to +80 mV for 18 ms with a 0.6-ms recovery period at −100 mV. Holding potential: −100 mV. Temperature: 5°C. Axon: DNAG141B.

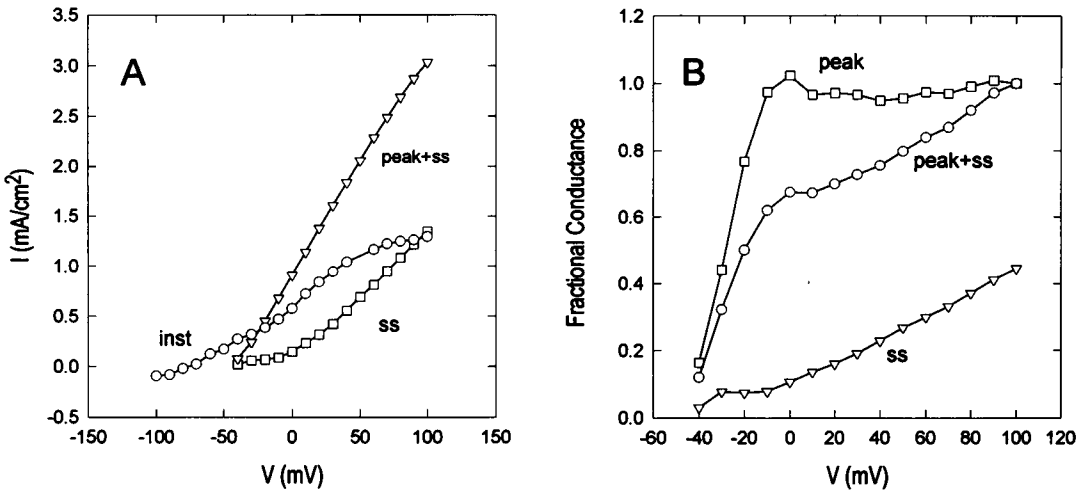

FIGURE 2 Current voltage relations at the peak (I_{peak}) and at the end of the pulse (I_{ss}). (*A*) Current values at the peak of the outward sodium current (peak + ss), at the end of the pulse (ss) and instantaneous I-V from an axon dialyzed in 178 Na^+-93 Cs^+. Same experiment as Fig. 1. (*B*) Fractional conductance at the peak and at steady state. Axon: DNAG141B.

the peak I-V is basically linear for the range of potentials tested. The values shown are the magnitude of the ionic currents at the peak, which include some of the steady-state pedestal, hence the name $I_{peak+ss}$. The I_{ss} displays more of a sigmoidal I-V relation. At negative potentials, virtually no current is found at the end of the pulse; at potentials more positive than 0 mV, a linear component develops that has a shallower voltage dependence than $I_{peak+ss}$. The instantaneous I-V (I_i) displays saturation at both ends of the voltage range tested but is linear for most of the range studied. The curves shown in Fig. 2 *B* were constructed using the data from Fig. 2 *A*. The fractional conductances (computed as I_{ss}/I_i, or $I_{peak+ss}/I_i$) are plotted as a function of pulse potential for I_{ss} and for $I_{peak+ss}$. From these the fractional conductance for the peak current alone (I_{peak}) was calculated and is also plotted in Fig. 2 *B*. These curves show that the fractional peak conductance or the probability of opening at the peak of the Na^+ current is highly voltage dependent at negative potentials, and that it reaches saturation at about −20 mV. The conductance at steady state is proportionally much smaller than that at the peak and displays very little voltage dependence at negative potentials; at positive potentials, it is more conspicuous and displays a shallow, almost linear voltage dependence. No saturation of I_{ss} was seen in this or in other similar experiments up to +120 mV.

The characteristics of the macroscopic inactivation could reflect the presence of two components in the sodium conductance: one that inactivates normally and another that does not inactivate. Alternatively, it could also be that the sodium conductance behaves differently at these extreme potentials (influenced perhaps by the presence of high sodium inside) and that inactivation was then not complete. To discriminate between the two explanations, we proceeded to dissect the two components at the macroscopic level. It was expected that the inactivating part of the current would be affected by the previous history of the channels, in particular, by charge immobilization due to a previous depolarization. It was unclear whether or not the steady-state component would sense the pre-depolarization. To look at the effect of the previous history on the sodium conductance, the membrane was subjected to pulse protocols involving depolarizing prepulses. The results are shown in the bottom part of Fig. 1 and also in Fig. 3. The set of records in Fig. 1 (*bottom*) was obtained in the same axon as those at the top part of the figure, pulsing to the same test potentials but applying an 18-ms prepulse to +80 mV with a 0.6-ms interval at −100 mV between the two pulses. With the prepulse, almost all of the inactivating component of the current was gone. I_{ss} stayed unaltered throughout the range of potentials tested. The two graphs in Fig. 3 further illustrate this point. In Fig. 3 *A* the I-V relations for $I_{peak+ss}$ and I_{ss} are plotted for currents between −40 mV and +100 mV. The circles represent the data in the absence of a prepulse; the triangles are data from the same axon subjected to the prepulse, in this case to +100 mV. The recovery period here was 1 ms long. It is obvious that the pre-depolarization affects almost exclusively the inactivating component of the current (*open triangles*) leaving the steady component unaffected (*filled triangles*). The graphs in Fig. 3 *B* illustrate the effect of the length of the prepulse on the magnitude of the ionic current for two different pulse potentials. As the prepulse was lengthened the peak component of the ionic current (*open symbols*) decayed, whereas again the I_{ss} (*filled symbols*) stayed constant. These results show that the prepulse did, in fact, affect more the inactivating part of the current.

An important factor in the manifestation of the prominent I_{ss} might be the high internal sodium concentration. From the results of Shoukimas and French (1980), in nonperfused axons it was expected that incomplete inactivation would persist irrespective of gradient orientation. To test this, the ionic currents were studied with a regular sodium gradient. Inward currents were recorded for a wide range of potentials. The

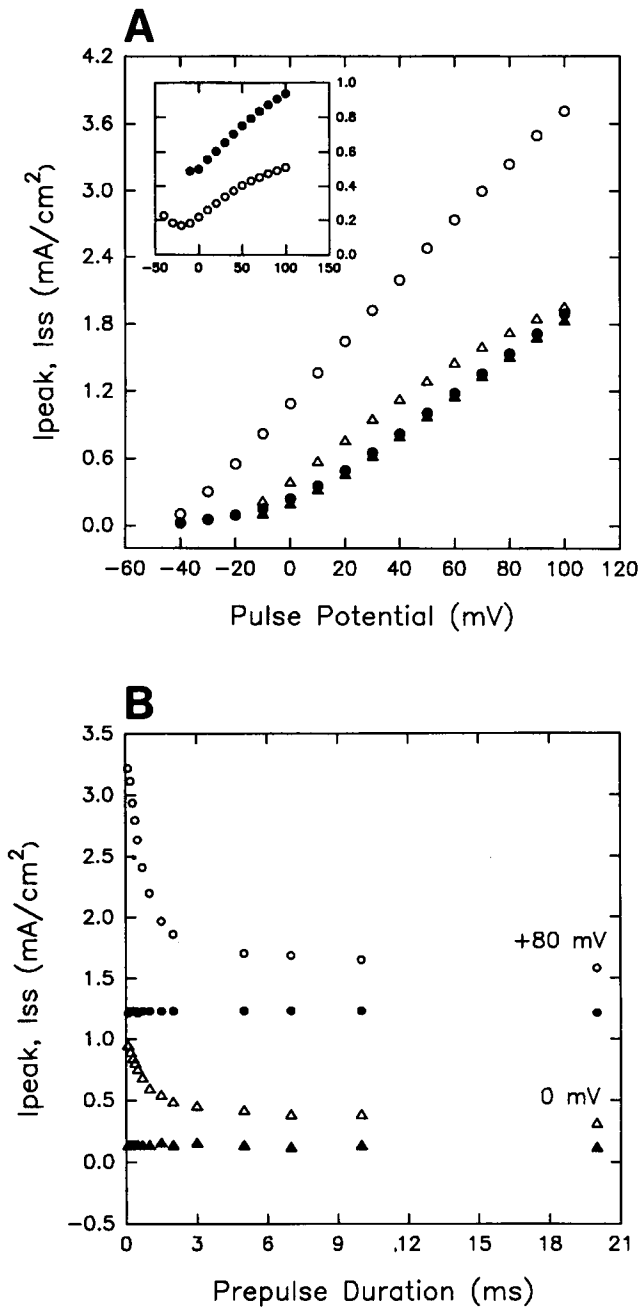

FIGURE 3 (*A*) Peak (*open symbols*) and steady-state (*filled symbols*) currents obtained with (*triangles*) and without (*circles*) an 18-ms prepulse to +100 mV. Inset: Ratio of I_{ss}/I_{peak} as a function of potential with (*filled symbols*) and without (*open symbols*) the prepulse. Interpulse period: 1 ms. Holding potential: −100 mV. The axon was dialyzed with 178 Na^+-93 Cs^+. External: 0 Na^+ CSW. Axon: DNAG091A. (*B*) Development of inactivation at two potentials: 0 mV (*triangles*) and +80 mV (*circles*) as a function of prepulse duration in ms. Open symbols are the values of the peak current, and filled symbols are the steady-state level. The prepulse is to +80 mV (18 ms). The interpulse duration was fixed at 1 ms. Holding and recovery potential: −100 mV. Solutions: 0 Na^+ CSW//178 Na^+-93 Cs^+. Axon: DNAG091B.

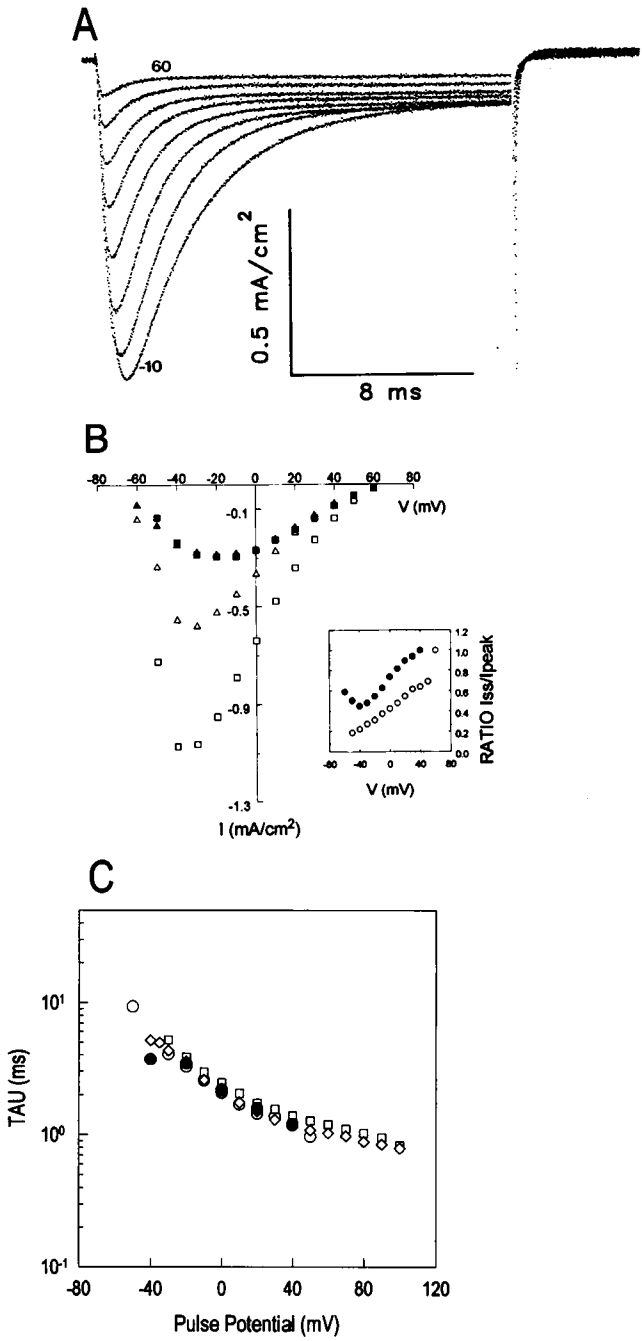

FIGURE 4 Inward sodium currents. (*A*) Family of records between −10 mV and +60 mV obtained in 108 Na^+//Internal Cs^+ gating. Axon: DNAG151B. (*B*) Peak (*open symbols*) and steady-state (*filled symbols*) currents as a function of potential. Triangles and squares are data with and without an 18-ms prepulse to +100 mV. The interpulse period is 1 ms at −100 mV. Holding potential: −100 mV. The inset is the ratio of steady-state current to peak current as a function of potential with (*filled symbols*) and without (*open symbols*) the prepulse. (*C*) Time constants of macroscopic inactivation as a function of potential. The decays of the macroscopic currents from recordings of inward (*circles*) and outward (*squares* and *diamonds*) currents were fitted to single exponentials. Data from 3 axons: DNAG081B (108 Na^+//Internal NMG^+ gating), DNAG091A, and DNAG091B (0 Na^+ CSW//178 Na^+-93 Cs^+).

superimposed currents shown in Fig. 4 *A* were obtained in an external solution containing 108 mM Na^+ in an axon dialyzed with a zero Na^+ internal medium. The currents shown were elicited with 18-ms pulses to potentials from

−10 to +60 mV. Under these conditions, the inward sodium currents also exhibited a nonzero I_{ss} already evident at −10 mV. Inactivation is however more complete at −10 mV than at +60 mV. The peak I-V curves shown in Fig. 4 *B* are fairly typical for inward currents. The steady-state level I-V is also shown in filled circles and amounted to 20 and 30% of the current at the peak of the I-V. The triangles represent the I-V relations at the peak and at a steady state of inward currents from the same axon for pulses preceded by a depolarizing prepulse to +100 mV. As was the case for the outward currents (Fig. 3), the pre-depolarization decreased $I_{peak+ss}$ without an appreciable effect on I_{ss}. The inset shows the ratio $I_{ss}/I_{peak+ss}$, indicating that at potentials more positive than −40 mV, the proportion of the remnant sodium current increases linearly with voltage, the proportion being greater all along the voltage range for the currents after depolarizing prepulses.

In Fig. 4 *C* are the time constants of fits to single exponentials of the decay of the ionic currents from experiments of inward and outward currents along with the corresponding data from prepulse experiments (see figure legend for explanation of symbols). There were no significant differences in the τs for macroscopic inactivation notwithstanding the opposite direction of the currents, which indicates that fast inactivation proceeds normally for outward currents as for inward currents. The results from these experiments are consistent with those of Shoukimas and French (1980) and ruled out the presence of high internal sodium as the cause of the persistent steady-state current.

Finally, additional information was provided by tail current experiments. In these, the depolarizing pulse duration was varied between 100 μs and 18 ms, and the currents developed upon repolarization were recorded. The experiments were done with a normal gradient (108 Na^+//0 Na^+) to record reasonably sized tail currents. In Fig. 5 *A–C* are the results of the analysis of two such protocols for test depolarizations to +80 mV and to 0 mV. The time course of the tail currents was fitted to two exponentials. The coefficients for each exponential component (fast and slow) are plotted in Fig. 5, *A* and *B* for +80 mV and 0 mV, respectively. In both graphs the squares represent the sum of the coefficients. In open and filled symbols of the same kind are the data for the fast and slow components, respectively. The features to note are, first, that the time course of the sum of the two coefficients at the two potentials, reproduces the time course of the ionic current during the depolarization. This is particularly important in the case of +80 mV, because the actual ionic current during the pulse was very small. So, with the tails we reproduced the time course of the conductance even in the absence of significant ionic flow during the pulse and still showed the incomplete inactivation pattern seen in the ionic currents. Therefore, this further emphasizes that incomplete inactivation is an intrinsic property of the conductance not depending on ion flow. Secondly, after an 18-ms depolarization, both at 0 and +80 mV, the coefficients approach each other, i.e., the weight of the exponentials is the same. Equality of coefficients is established very early at +80 mV depolarizations, from 5 ms on. At 0 mV it takes longer. The peak contribution of the fast component happens at about the same time as the peak of the conductance. The

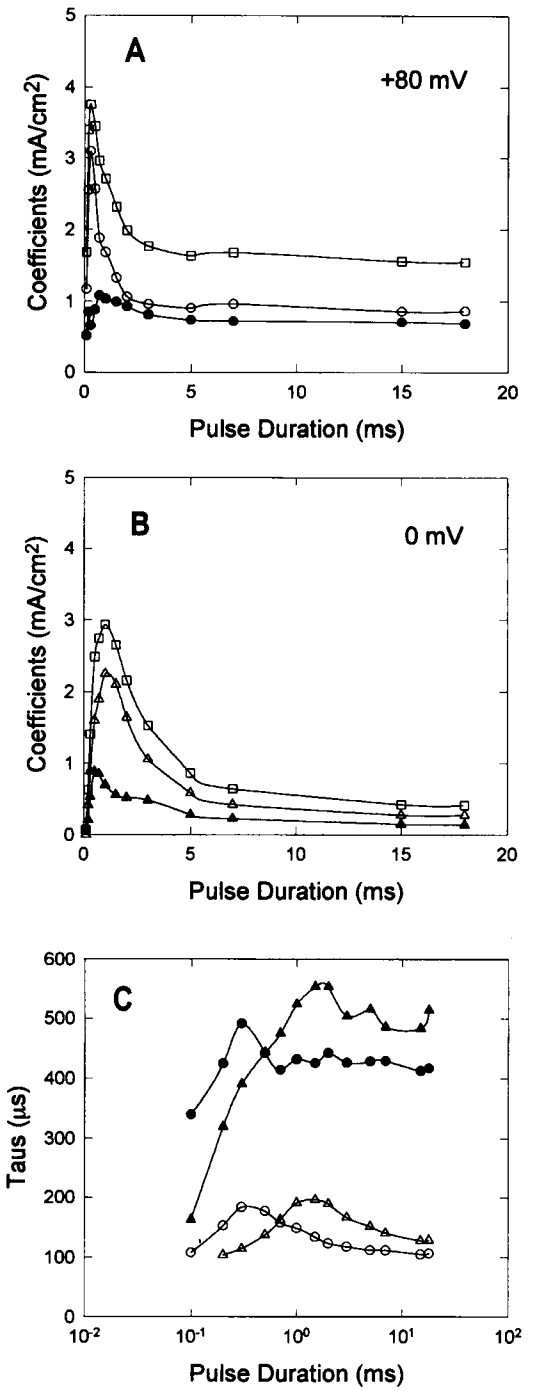

FIGURE 5 Two relaxations in the tail currents and the dependence on pulse duration. The time course of tail currents at −70 mV from pulses to 0 and +80 mV were fitted to 2 exponentials. The coefficients of each of the components are plotted in open and closed symbols of the same kind in (*A*) (+80 mV pulses) and (*B*) (0 mV pulses) as functions of pulse duration. The squares in plots are the sum of the two coefficients at each pulse duration. (*C*) The semilogarithmic plot of the corresponding time constants, in μs (*circles* for the τs at +80 mV and *triangles* for the τs at 0 mV), as functions of pulse duration. Axon:DNAG151B.

slow component is smaller and apparently peaks earlier than the fast component. The levels acquired after an 18-ms pulse to 0 and +80 mV, compared with the respective peak values after 1 and 0.3 ms, were 14 and 41%, respectively. For comparison with the ionic current at 0 mV, the steady-state level at 18 ms was 19% of the peak that happened at 0.95 ms. At +80 mV the current was too small to make the corresponding measurement. From the data from other axons, levels between 40 and 50% were found. In Fig. 5 *C* are the corresponding time constants obtained from the fits. In circles are data at +80 mV, and in triangles are data at 0 mV. For both potentials the fast time constant shows a bell-shaped behavior. The peaks again happened close to the peaks in the conductance (see parts A and B). The slow time constants were constant for most of the pulse durations. A gradual increase with pulse duration, particularly evident for the data at 0 mV, was observed. As will be discussed further in the next section, the time constants are not expected to change in a Markovian system. It is possible that more than two exponentials would represent the data better and that the values of the time constants we got are a combination of others. Thus the time course observed. Although a double exponential relaxation in the tails may arise from a single open-state model depending on the proportions of the rate constants and state of occupancy at each state (see for example, Goldman, 1991; Bezanilla et al., 1994), in this case the traditional expectation from a double relaxation tail of two open states is very likely the case, as will be demonstrated at the single-channel level in the accompanying paper.

Gating currents

An important tool in the study of the gating of sodium channels under various conditions is the examination of their gating currents, i.e., the charge moved in response to the change in the membrane field that occurs with a depolarization. Fig. 6 shows superimposed records of ionic (*top*) and "on" gating currents (*bottom*) obtained with and without a prepulse to +80 mV. The test potential was +80 mV. As seen in the previous figures, the inactivating component of the sodium current is almost completely eliminated by the prepulse, whereas the steady-state component stayed unchanged. The gating currents showed a short rising phase followed by a relaxation with at least two components. With the prepulse, along with a reduction in the amount of charge moved, there was an apparent preferential depression of the slow component of the gating current. The suppression of the slower component of the 'on' gating has been previously reported for this and other preparations (see Starkus and Rayner, 1991; Armstrong and Bezanilla, 1977). In Fig. 7 the "on" gating charge is plotted as a function of potential. Without a prepulse (*filled symbols*) the charge moved exhibited close to sigmoidal behavior with its major voltage dependence in the range between −90 and −20 mV. At potentials more positive than zero the charge reached saturation. When the test pulse was preceded by a prepulse followed by a brief recovery period of 1 ms at −100 mV, the total 'on' charge moved at the onset of the test pulse was smaller along all the voltage range. The maximum charge moved by the test pulse was only about 50% of the charge moved without a prepulse. The reduction in total charge is expected from the development of charge immobilization during the first pulse, the interpulse repolarization period not being long enough to fully recover the charge. Because the recovery potential was considerably hyperpolarized (−100 mV) more than ⅓ of the charge was available after 1 ms. In fact, the charge returning after 1 ms at −100 mV was found to be around 50–60% of the total. Returns to less negative potentials like −70 mV, for the same period, remobilized significantly less charge (not shown). At very positive potentials, after the apparent saturation level is reached (at around 0 mV), there is an additional, progressive decline in the total charge moved by the second pulse.

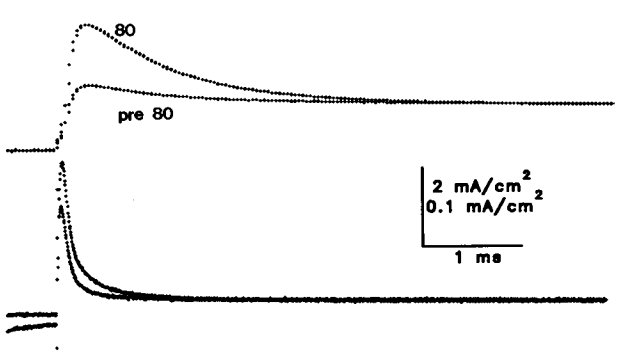

FIGURE 6 Top: Ionic outward currents from a pulse to +80 mV, with and without a depolarizing prepulse to +80 mV. Solutions: 0 Na^+ CSW//178 Na^+-93 Cs^+. Bottom: corresponding 'on' gating currents. Same conditions as the top but with 1 μM external TTX. Axon: DNAG091B.

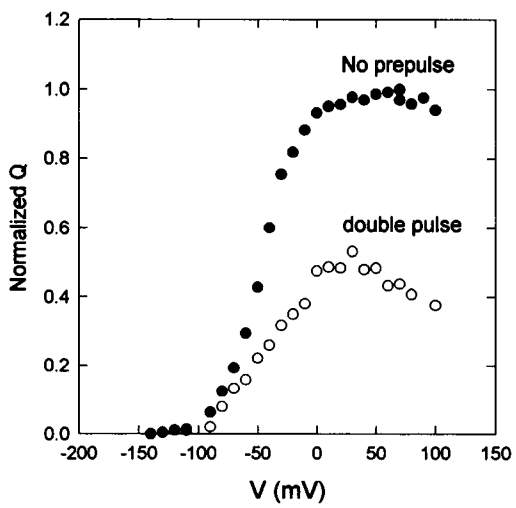

FIGURE 7 Normalized total 'on' gating charge as a function of potential. Filled circles are data in the absence of a prepulse. Open circles are the charged moved after an 18-ms prepulse to the same potential as the test pulse in the abscissa. Recovery at −100 mV for 1 ms. Holding potential: −100 mV. Solutions: 0 Na^+ CSW + 1 μM TTX//Internal NMG^+ gating. Axon: DNAG081B.

The manifestation of fast inactivation in gating current measurements has been linked to charge immobilization (Armstrong and Bezanilla, 1977). As fast inactivation proceeds, so does charge immobilization with the same voltage dependence. In the squid sodium channel, the 'on' gating currents do not contain a component that can be readily identified with inactivation. We looked for evidence of charge movement associated with the noninactivating component of the current by studying the development of inactivation as well as the kinetics of the 'on' gating currents at very positive potentials. We specifically looked for a significant nonimmobilizable portion of the charge or, alternatively, movement of the gating charge developing with extreme depolarization. In Fig. 8 the ratios of the charge moved upon repolarization to that moved with the depolarization are plotted as a function of pulse duration for pulses to 0 and +80 mV. The off/on ratio decreased with time of depolarization for both potentials, as expected for charge immobilization by inactivation. At +80 mV the charge is immobilized faster, as expected, from faster kinetics of inactivation at this potential, but it reached the same steady level as at 0 mV. This result shows that the amount of charge immobilized by a pulse to +80 mV is the same as the amount immobilized by a pulse to 0 mV. To see to what extent there were differences in the return of the gating charge between mild and strong depolarizations, the charge moved with repolarization was broken down into its two most apparent components. The plots shown in Fig. 9, *A* and *B* give the relative charge as a function of time during the pulse. The ratios of the charge returning with fast kinetics are in open symbols, and the ratios of the charge returning with slower kinetics are in filled symbols. At both potentials, there was no charge immobilization with very short pulses; the charge returned mainly through a fast route. As depolarization takes its course more charge gets immobilized and returns with slower kinetics. The onset of charge immobilization takes place earlier for the depolarization to +100 mV. After around 1 ms, only 30–40% of the charge returns with fast kinetics. About the same percentage of charge returning with fast kinetics is seen at 0 mV, but only after around 5 ms. These results are crucial, because they indicate that the process of inactivation, as revealed by charge immobilization and decay of the macroscopic current, is taking place normally. The time dependence of charge immobilization and the proportion of charge being immobilized agree well with those expected for normal fast inactivation. The fact that there exists a remnant ionic current at the end of the pulse and that there still is normal charge immobilization suggests that the noninactivating component of the current comes from channels opening from the inactivated state. The alternative is, of course, that at very positive potentials the steady-state current is carried by another channel species with very little if any charge associated with

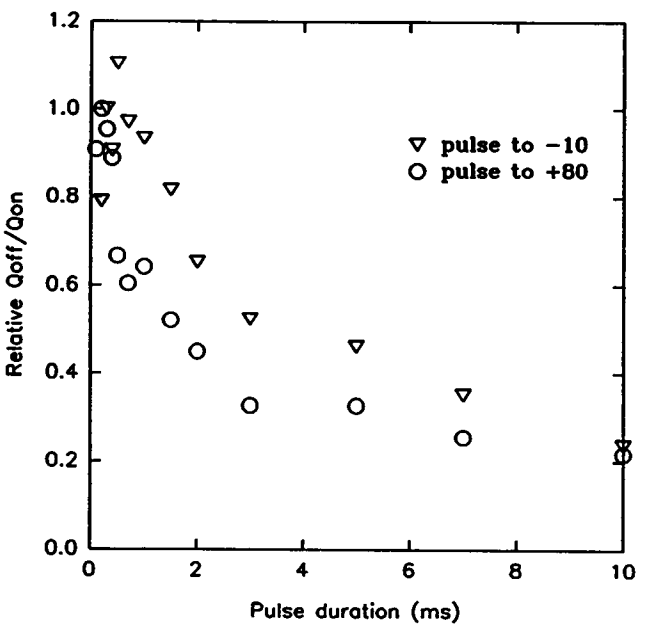

FIGURE 8 Charge immobilization. The ratios of 'off' gating, at −70 mV, to 'on' gating charge are plotted as a function of the duration of the test pulse, in ms. Inverted triangles are data going to 0 mV, and circles, to +80 mV. Holding potential: −100 mV. Solutions: 0 Na^+ CSW + 1 μM TTX//178 Na^+-93 Cs^+. Axon: DNAG161A.

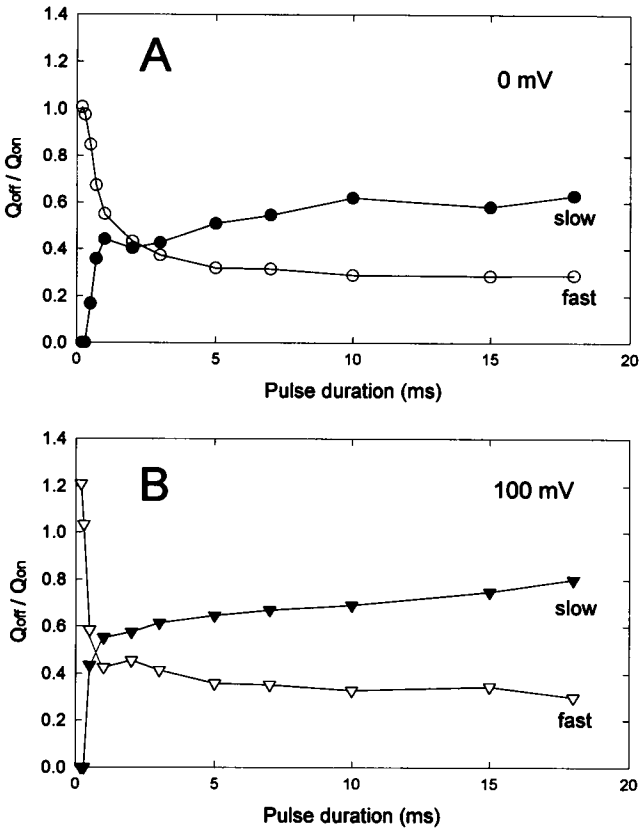

FIGURE 9 Development of inactivation. (*A*) Charge immobilization at 0 mV. (*B*) Charge immobilization at +100 mV. The off gating was fitted to two exponentials and the charge corresponding to each component was divided by the total 'on' gating charge. The resulting ratios off/on are plotted as a function of pulse duration. Before and after the test pulses to 0 or +80 mV the membrane was held at −120 mV for 20 ms and 30 ms, respectively. Holding potential: −100 mV. Axon: DNAG051B. Solutions: 0 Na^+ CSW + 1 μM TTX//178 Na^+-93 Cs^+.

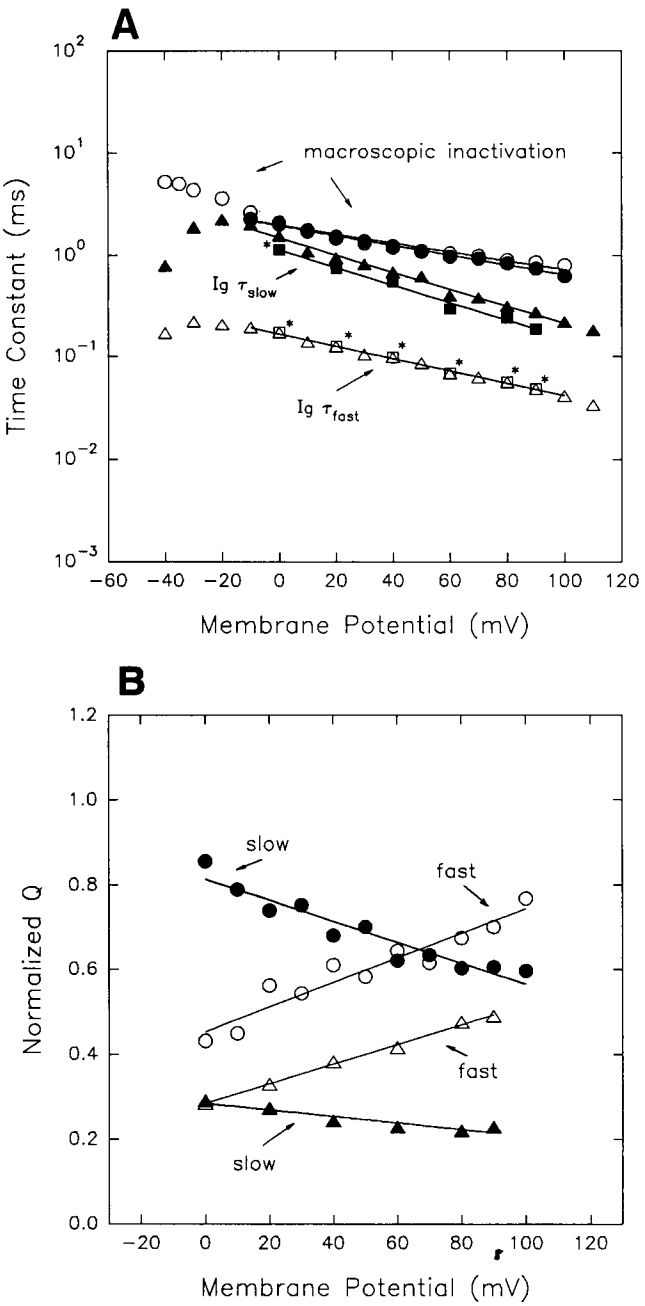

FIGURE 10 Analysis of the components of the relaxations of the 'on' gating currents. (*A*) The fitted values of τ_{fast} and τ_{slow} of the 'on' gating currents are in triangles. The values after application of a prepulse are in squares. The asterisks denote values of τ that were maintained fixed for the fit to the data obtained with prepulses. The values are plotted as a function of pulse potential. The values given are those for the best fits to the data, even in the case of fixed values of τ. Also shown are the time constants of the decay of the ionic currents for the same axon in the presence (●) or absence (○) of a prepulse. The prepulse was to +80 mV for 18 ms. The interpulse was to −100 mV for 1 ms. Data in the range between 0 and +100 mV were fitted to an exponential function of voltage. The slopes gave an e-fold decay for 99 (○) and 90.5 mV (●) for the time constants of ionic inactivation. The τs from the fast and slow relaxations of the 'on' gating currents changed e-fold for 72.3 (△), 51 (▲), and 49.6 mV (■). (*B*) Areas of the fast and slow components of the 'on' gating charge as a function of pulse potentials. The data without a prepulse are in circles, and data with a prepulse are in triangles . Filled symbols are from the slow components, and the empty symbols are from the fast components. Linear regressions between 0 and +100 mV gave the following slopes: −4.4 (●), 6.12 (○), −1.62 (▲), and 4.8 (△). Axon: DNAG091B. Holding potential: −100 mV. Solutions: 0 Na^+ CSW + 1 μM TTX//178 Na^+-93 Cs^+.

its opening and closing. All the gating charge would then come from the inactivating sodium current.

The kinetics of the 'on' gating current were compared with the kinetics of macroscopic ionic inactivation. The decay of the 'on' gating current was fitted to two exponentials. The fitted time constants are plotted as triangles in Fig. 9 *A* as a function of potential: open symbols are τ_{fast}, and filled symbols are τ_{slow}. Squares represent the values of both relaxation time constants (τ_{slow} and τ_{fast}) in the same axon after depolarizing prepulses to +80 mV followed by 1-ms recovery periods at −100 mV. The fit to the data from currents with the prepulses was done either (i) letting all the parameters free, or (ii) fixing the values of τ_{fast} and/or τ_{slow} to the values obtained from the gating currents without a prepulse and/or obtained from the free fit of the data with a prepulse. The values plotted were always those from the best fit. The asterisks indicate the values kept fixed during the fitting procedure. As can be seen, the best fits to the data with the double-pulse protocol were consistently obtained when τ_{fast} was fixed at the value obtained for the single-pulse experiment, indicating that this gating component was still present but that the total charge moved with these kinetics was greatly reduced by the application of the prepulse (see Fig. 9 *B*). The slow component, on the other hand, was well fit with time constants slightly smaller than in the single-pulse protocol. In both cases, the voltage dependence of τ_{fast} and τ_{slow}, were unchanged by the pre-depolarization. For comparison, the time constants of decay of the ionic currents for the same axon are also plotted. The open circles are from single-pulse protocols, and the filled symbols are from double-pulse protocols. The prepulse did not affect the voltage dependence of the inactivation time constant. The results show that neither the magnitude nor the voltage dependence of the time course of ionic inactivation coincide with the values of τ obtained from the best fits to the gating current data. This means that also at very positive potentials there is no evident component of the gating currents associated with macroscopic inactivation. It also implies that the process that determines the development of the noninactivating component does not carry a measurable amount of charge, in agreement with the shallow voltage dependence of I_{ss} seen in Fig. 2.

The charge moved by each gating component is plotted in Fig. 10 *B*. The fast gating components are in open symbols, and the slow components are in filled symbols. In circles are data from single-pulse protocols, and in triangles, data with prepulses. With and without a prepulse, the voltage dependence of the slow component was shallower than and inverse to that of the fast component. Both fast and slow components of the gating currents were dramatically reduced by the prepulse (charge immobilization), but the effect was apparently

greater for the slow component, as was hinted by visual inspection of the traces in Fig. 6 (*bottom*). In fact, after appropriate scaling of the peak of the gating currents, the fast component superimposed, whereas the slow component seems greatly reduced (data not shown). There was no obvious effect of the prepulse on the voltage dependence of either component.

DISCUSSION

Inactivating versus noninactivating components

It seems consistent that the squid giant axon sodium channel behaves slightly different than other sodium channels, in that inactivation is not complete, particularly at positive potentials. In neuroblastoma N1E115 cells, for instance, Aldrich et al. (1983) reported that the time course of currents reproduced from single-channel data is basically determined by the rate of activation and that inactivation was complete. In cloned rat brain II sodium channels, either in transfected mammalian cells (West et al., 1992) or in *Xenopus* oocytes coexpressed with the β_1 subunit (Isom et al., 1992), inactivation has been found to be fast and more complete. The sodium currents recorded in patches from *Electrophorus* electrocytes show complete inactivation even at very positive potentials (Shenkel and Bezanilla, 1991). In the squid, this is clearly not the case in the macroscopic currents, and, as will be demonstrated in the accompanying paper (Correa and Bezanilla, 1994), neither is it the case at the single-channel level. The usual range of potentials at which sodium currents can be accurately studied under conditions as physiological as possible extends from resting to about +20 mV before getting to a range close to the reversal potential where the currents become very small. Even at +20 mV, however, sodium currents never came back to baseline levels. Imposition of an inverse sodium gradient allowed an extention of the range of potentials. As was pointed out previously by other investigators (Chandler and Meves, 1970a–c; Shoukimas and French, 1980; Keynes et al., 1992a, b), the level acquired by the current at the end of the pulse becomes more prominent with depolarization. There are certain characteristics of the inactivating portion of the current that differ from those of the noninactivating component. As expected, the transient component is very sensitive to previous depolarization. Inactivation affects the development of succeeding currents when recovery from it is not complete. The steady-current component was not visibly altered by the prepulses, indicating that either it follows a parallel route that is accessed with depolarization and consequently becomes independent or that it is a totally different conductance. The brief repolarizations of around 1 ms to very negative potentials (−100 mV) were probably enough for this component to recover from the prepulses, whereas they were not long enough for the inactivating component. In addition, it is clear that the voltage dependence of the two components is also different. The fractional current at the peak had a much steeper relation with voltage than that of the noninactivating portion. Also, Keynes et al. (1992a) have reported different temperature coefficients of the permeability properties of both components and differential effects of ions on the currents themselves. On the other hand, there are similarities that are more related to the single-channel characteristics pointing to a single-channel entity, as will be shown in the accompanying paper (Correa and Bezanilla, 1994).

High internal sodium

The development of the noninactivating component does not depend on the presence of high concentrations of sodium in the inside, inasmuch as it is also visible with normal gradients and in nonperfused axons (Shoukimas and French, 1980). It amounts to about 30% of the maximum peak sodium current. The ratio of noninactivating current to peak current was found to increase monotonically with voltage for inward and outward currents. The effect of depolarizing prepulses was similar to that found with inverted sodium gradients: the peak was depressed, and the steady current stayed unchanged. The time course and voltage dependence of macroscopic fast inactivation did not depend on the orientation of the gradient. The time constants obtained from fits to single exponentials were of the same magnitude and overlapped in the voltage range, indicating again that the process of inactivation follows its course irrespective of gradient orientation. In their original thorough study of outward sodium currents in the squid giant axon, Chandler and Meves (1970a–c) suggested that a plausible explanation for the incomplete inactivation could be modulation of the conductance by high internal sodium by direct interaction of sodium ions with the inactivation mechanism (gate) interfering with the block. Different ions, usually used to replace potassium in the internal medium, affect inactivation by slowing down the rate of decay of the macroscopic current (Oxford and Yeh, 1985; Goldman, 1988; Keynes and Meves, 1993). A well documented case is that of quaternary amines, in particular, TEA and tetramethylammonium (Oxford and Yeh, 1985; Keynes et al., 1992a, b; Keynes and Meves, 1993). In the case of high internal sodium, more than a slowing down of the rate of inactivation, what we see is a remnant current. In addition, fast inactivation, as mentioned above, seems to be following the same trend in inward and outward currents.

The gating and ionic current recordings were done in the presence of some internal TEA, which was used to block any residual potassium conductance. Although the maximum concentration used was only 50 mM, some slowing down of fast inactivation could result, and this could add to the steady-state current seen. The ratios of I_{ss}/I_{peak} reported here are, however, comparable to those found previously in nonperfused axons (Shoukimas and French, 1980) or in axons perfused with higher sodium concentrations (Chandler and Meves, 1970a) but differ by a factor of two from those obtained in Cs^+ perfused axons (Shoukimas and French, 1980). Furthermore, the time course of the tail currents after pulses

of different lengths reproduce closely the time course of the sodium conductance at the test potential. This, in the particular case of almost zero ionic current, is an indication of independence of the conductance on the direction of current flow.

The time constants of relaxation of the tail currents showed a dependence on the length of the pre-depolarization. This was particularly the case for those of the fast process where we found a bell-shaped relation with pulse duration, the peak of the bell closely matching the maximum of the conductance. In the case of the slow component, an increase in the time constants with test pulse duration was evident for the data at 0 mV and not as clear for +80 mV. Although we have not attempted fitting all the tail currents to more than two exponentials, we believe that the time course we observe in the fitted values is a consequence of averaging time constants from several components. The weights of the components would vary with the initial conditions set by the point in time during the pre-depolarization when the repolarization is initiated. An alternative would be, however, that the time constants of the components do actually vary depending on the pulse duration, in which case the system would be clearly non-Markovian.

Gating currents

The macroscopic ionic data suggest that inactivation is impaired at positive potentials in that it does not proceed to completion at least from a traditional Hodgkin and Huxley type view. Our results with gating currents show that inactivation actually takes place normally, that it has the normal voltage dependence, and that charge immobilization occurs regardless of the fact that there is a significant remnant current. As expected, the time course of charge immobilization was faster for extreme potentials (+80 and +100 mV) as compared with smaller depolarizations (0 mV). However, regardless of the magnitude of the depolarization, the amount of immobilized charge is the same, although the amount of apparent inactivation of the macroscopic ionic current decreased significantly with depolarization. This favors a common pathway for activation and inactivation at all potentials and suggests that the access to the hypothetical second open state would have to be *via* an inactivated state.

CONCLUSION

We have provided here basic information on kinetics of sodium channels at very positive potentials. Macroscopic and gating current experiments were designed to look more closely at the noninactivating component of the macroscopic sodium currents at these potentials. It is possible to separate the inactivating and noninactivating components in the macroscopic ionic current, but the separation is not obvious in the gating currents. In fact, the charge immobilization results indicate that inactivation is normal and that one must think of a second conductance appearing at positive potentials. In the accompanying paper we show that this second conductance is a second open state of the same sodium channel. The results presented here will be critical to constrain the connection of this second open state to the rest of the kinetic model of the Na^+ channel.

ACKNOWLEDGMENT

This work was supported by USPHS grant GM 30376.

REFERENCES

Adelman, W. J., and J. P. Senft. 1966. Effects of internal sodium ions on ionic conductance of internally perfused axons. *Nature.* 212:614–616.

Aldrich, R. W., D. P. Corey, and C. F. Stevens. 1983. A reinterpretation of mammalian sodium channel gating based on single channel recording. *Nature.* 306:436–441.

Armstrong, C. M., and F. Bezanilla. 1977. Inactivation of the sodium channel. II. Gating current experiments. *J. Gen. Physiol.* 70:567–590.

Bezanilla, F. 1987. Single sodium channels from the squid giant axon. *Biophys. J.* 52:1087–1090.

Bezanilla, F., and C. M. Armstrong. 1977. Inactivation of the sodium channel. I. Sodium current experiments. *J. Gen. Physiol.* 70:549–566.

Bezanilla, F., and A. M. Correa. 1991. Single sodium channels in high internal sodium in the squid giant axon. *Biophys. J.* 59:12a.

Bezanilla, F., E. Perozo, and E. Stefani. 1994. The gating of Shaker K^+ channels. II. The components of gating currents. *Biophys. J.* In Press.

Chandler, W. K., and H. Meves. 1970a. Sodium and potassium currents in squid axons perfused with fluoride solutions. *J. Physiol.* 211: 623–652.

Chandler, W. K., and H. Meves. 1970b. Evidence for two types of sodium conductance in axons perfused with sodium fluoride solution. *J. Physiol.* 211:653–678.

Chandler, W. K., and H. Meves. 1970c. Rate constants associated with changes in sodium conductance in axons perfused with sodium fluoride. *J. Physiol.* 211:679–705.

Correa, A. M., and F. Bezanilla. 1994. Gating of the squid sodium channel at positive potentials. II. Single channels reveal two open states. *Biophys. J.* 66:1864–1878.

Goldman, L. 1988. Internal cations, membrane current, and sodium inactivation gate closure in *Myxicola* giant axons. *Biophys. J.* 54: 1027–1038.

Goldman, L. 1991. Gating current kinetics in *Myxicola* giant axons. Order of the back transition rate constants. *Biophys. J.* 59:574–589.

Hamill, O. P., A. Marty, E. Neher, B. Sackmann, and F. Sigworth. 1981. Improved patch clamp techniques for high resolution current recording from cells and from cell-free membrane patches. *Pfluegers Arch. Eur. J. Physiol.* 381:85–100.

Hodgkin, A. L., and A. F. Huxley. 1952. A quantitative description of membrane current and its application to conduction and excitation in nerve. *J. Physiol.* 117:500–544.

Horn, R., and C. A. Vandenberg. 1984. Statistical properties of single sodium channels. *J. Gen. Physiol.* 84:505–534.

Isom, L. L., K. S. De Jongh, D. E. Patton, B. F. X. Reber, J. Offord, H. Charbonneau, K. Walsh, A. L. Goldin, and W. A. Catterall. 1992. Primary structure and functional expression of the 61 subunit of the rat brain sodium channel. *Science.* 256:839–842.

Keynes, R. D., N. G. Greeff, and I. C. Forster. 1992b. Activation, inactivation and recovery in the sodium channels of the squid giant axon dialysed with different solutions. *Philos. Trans. R. Soc. Lond. B. Biol. Sci.* 337:471–484.

Keynes, R. D., and H. Meves. 1993. Properties of the voltage sensor for the opening and closing of the sodium channels in the squid giant axon. *Proc. R. Soc. Lond. B. Biol. Sci.* 253:61–68.

Keynes, R. D., H. Meves, and D. Hof. 1992a. The dual effect of internal tetramethylammonium ions on the open states of the sodium channel in the squid giant axon. *Proc. R. Soc. Lond. B. Biol. Sci.* 249:101–106.

Nagy, K. 1987. Evidence for multiple open states of sodium channels in neuroblastoma cells. *J. Membr. Biol.* 96:251–262.

Nagy, K., Kiss, T., and D. Hof. 1983. Single Na channels in mouse neuroblastoma cell membrane. Indications for two open states. *Pfluegers Arch. Eur. J. Physiol.* 399:302–308.

Oxford, G. S., and J. Z. Yeh. 1985. Interactions of monovalent cations with sodium channels in the squid axon. I. Modification of physiological inactivation gating. *J. Gen. Physiol.* 85:583–602.

Perozo, E., F. Bezanilla, and R. Dipolo. 1989. Modulation of K channels in dialyzed squid axons. ATP-mediated phosphorylation. *J. Gen. Physiol.* 93:1195–1218.

Quandt, F., and T. Narahashi. 1982. Modification of single channels by batrachotoxin. *Proc. Natl. Acad. Sci. USA.* 79:6732–6736.

Scanley, B. E., D. A. Hanck, T. Chay, and H. A. Fozzard. 1990. Kinetic analysis of single sodium channels from canine cardiac purkinje cells. *J. Gen. Physiol.* 95:411–437.

Shenkel, S., and F. Bezanilla. 1991. Patch recordings from the electrocytes of Electrophorus. Na channel gating currents. *J. Gen. Physiol.* 98: 465–478.

Shoukimas, J. J., and R. J. French. 1980. Incomplete inactivation of sodium currents in nonperfused squid axons. *Biophys. J.* 32:857–862.

Sigworth, F. 1981. Covariance of nonstationary sodium current fluctuations at the Node of Ranvier. *Biophys. J.* 34:111–133.

Starkus, J. G., and M. D. Rayner. 1991. Gating current "fractionation" in crayfish giant axons. *Biophys. J.* 60:1101–1119.

Stimers, J. R., F. Bezanilla, and R. E. Taylor. 1985. Sodium channel activation in the squid giant axon. Steady state properties. *J. Gen. Physiol.* 85:65–82.

Vandenberg, C. A., and F. Bezanilla. 1991a. A sodium channel model based on single channel, macroscopic ionic, and gating currents in the squid giant axon. *Biophys. J.* 60:1511–1533.

Vandenberg, C. A., and F. Bezanilla. 1991b. Single-channel, macroscopic, and gating currents from sodium channels in the squid giant axon. *Biophys. J.* 60:1499–1510.

West, J. W., D. E. Patton, T. Scheuer, Y. Wang, A. L. Goldin, and W. A. Catterall. 1992. A cluster of hydrophobic amino acid residues required for fast Na^+-channel inactivation. *Proc. Natl. Acad. Sci. USA.* 89: 10910–10914.